

CONSTRAINING EVOLUTION IN THE HALO MODEL USING GALAXY REDSHIFT SURVEYS

RENBIN YAN¹, DARREN S. MADGWICK^{1,2} & MARTIN WHITE^{1,2,3}

¹ Department of Astronomy, University of California, Berkeley, CA 94720

² Lawrence Berkeley National Laboratory, Berkeley, CA 94720

³ Department of Physics, University of California, Berkeley, CA 94720

Draft version November 9, 2018

ABSTRACT

We use the latest observations from the 2dF Galaxy Redshift Survey to fit the conditional luminosity function (CLF) formulation of the halo-model for galaxies at $z = 0$. This fit is then used to test the extent of evolution in the halo occupation distribution (HOD) to $z = 0.8$, by comparing the predicted clustering from this CLF to preliminary results from the DEEP2 Redshift Survey. We show that the current observations from the DEEP2 Redshift Survey are remarkably consistent with no evolution in the CLF from $z = 0$ to $z = 0.8$. This result is surprising, in that it suggests that there has been very little change in the way galaxies occupy their host dark matter halos over half the age of the Universe. We discuss in detail the observational constraints we have adopted and also the various different selection effects in each survey and how these impact on the galaxy populations encountered in each survey.

Subject headings: Galaxies: high-redshift — Cosmology: theory

1. INTRODUCTION

Despite impressive advances in many areas over the last decade, galaxy formation remains one of the central unsolved puzzles in cosmology. While it is now generally accepted that galaxies form within dark matter halos (White & Rees 1978), whose properties we know about with increasing reliability, the details of this process are only poorly understood. With the advent of large-scale surveys of galaxies and ever more sophisticated computer simulations of structure formation we need to develop a more nuanced view of galaxy formation than has been typical until now. Key to advances in this subject is a framework within which to compare theory and observations in as transparent a way as possible.

While studies of individual galaxies can shed light on many of the relevant physical processes which shape them, galaxy clustering stands as the most successful route to constraints on galaxy formation models to date. Thus we desire a framework within which we can interpret the numerous measurements of galaxy clustering that have accumulated over the years.

The ‘halo model’ provides such a framework. Building on the insights of semi-analytic galaxy formation (e.g. Kauffmann, White & Guiderdoni 1993; Cole et al. 1994; Somerville & Primack 1999) and high-resolution hydrodynamic simulations including star-formation and feedback (Katz, Hernquist & Weinberg 1999; Gardner et al. 2001; Pearce et al. 1999; White, Hernquist & Springel 2001; Yoshikawa et al. 2001) the halo model has been extensively developed in recent years, e.g. Jing, Mo & Borner. 1998; Benson et al. 2000; Seljak 2000; Peacock & Smith 2000; Ma & Fry 2000; Scoccimarro et al. 2001; White 2001; Scoccimarro & Sheth 2001; Berlind & Weinberg 2002; Scranton 2002; Yang, Mo & van den Bosch 2003; (see Cooray & Sheth 2002 for a recent review and references to the earlier literature).

The halo model postulates that all galaxies lie in virialized halos and that the number and type of galaxies in halos is determined primarily (or entirely) by the halo mass.

Knowledge of the number of galaxies as a function of halo mass, known as the halo occupation distribution (HOD), their spatial and velocity distribution within the halos and a model for the spatial clustering of dark matter halos is sufficient to predict most observables in large-scale structure. The halo model provides a new way of thinking about galaxy bias which is more physically informative than the earlier schemes. It also provides a conceptual division between ‘galaxy formation’ and ‘cosmology’ in that the latter affects the spatial distribution and number of dark matter halos, while the former describes the properties and number of galaxies which form within the halos. The key advantage of having this conceptual separation between halo and galaxy properties is that the evolution in the spatial distribution and number of dark matter halos can be well understood through the use of numerical simulations, allowing us to exclusively constrain galaxy formation processes with the use of recent large galaxy redshift surveys.

The recent completion of the 2dF Galaxy Redshift Survey (2dFGRS, Colless et al. 2001), together with the ongoing progress of the Sloan Digital Sky Survey (SDSS, Strauss et al. 2002), have heralded a new age of precision quantification in the galaxy population in the local ($z \sim 0$) Universe. The sheer size of these data sets enables a particularly accurate characterization of the properties of the galaxies themselves, together with how these galaxies are distributed with respect to each other. These two ingredients will be key to resolving many outstanding issues in galaxy formation and evolution. The DEEP2 Galaxy Redshift Survey (Davis et al. 2002) will herald a similar degree of improvement in our understanding of the galaxies at $z \sim 1$. The goal of this paper is to link these two significant advances in our understanding of the galaxy population, by performing an initial comparison between high fidelity 2dFGRS results and preliminary DEEP2 clustering results (Coil et al. 2003) within the halo-model framework.

We use the latest observations from the 2dFGRS to constrain the HOD at $z \sim 0$, by adopting the conditional luminosity function (CLF) formalism developed by Yang et al. (2003). We make use of a Markov-Chain Monte-Carlo

arXiv:astro-ph/0307248v2 18 Aug 2003

(MCMC; see Gilks, Richardson & Spiegelhalter 1996) procedure to explore the multi-dimensional parameter space of the CLF. At present we consider the cosmology to be fixed. Specifically we assume a Λ CDM model with $\Omega_m = 0.3$, $\Omega_\Lambda = 0.7$, $H_0 = 100 h \text{ km s}^{-1} \text{ Mpc}^{-1}$ with $h = 0.7$, $\Omega_B h^2 = 0.02$, $n = 0.95$ and $\sigma_8 = 0.9$ (close to the best fit to the CMB data for this cosmology). We note in passing that the matter power spectrum is insensitive to the precise value of $\Omega_B h^2$ assumed and that the normalization is well fixed by the recent WMAP data (Bennett et al. 2003) once a specific cosmology is chosen.

Once we have constrained the CLF at $z \sim 0$ in this way, we proceed to test the extent of evolution in the galaxy formation processes which are quantified by this function. In particular (by assuming a given cosmological model in our N-body simulations) we use this CLF to make predictions about observable galaxy properties at $z \sim 1$ – which are tested using the recent clustering observed in the DEEP2 Galaxy Redshift Survey (Coil et al. 2003).

The outline of this paper is as follows: In §2 we describe the conditional luminosity function formulation of the halo model and summarize the main parameters in this model. Section 3 gives a detailed description of all the observational constraints we will use in our analysis, and in particular describes how we deal with the different selection effects in the two surveys. Our fitting procedure is outlined in §4, which also discusses the best-fitting parameters output by the MCMC. In §5 we present our prediction for the clustering we would expect to see in the DEEP2 Redshift Survey if the CLF hadn't undergone any evolution, and then compare this to what is actually observed and we present our conclusions in §6.

2. THE CONDITIONAL LUMINOSITY FUNCTION

Here we briefly review the conditional luminosity function (CLF) formalism of Yang et al. (2003). Further details on the halo model and references to the literature can be found in Appendix A.

Typically when implementing the halo-model, the HOD is assumed to simply yield the probability of having N galaxies in a halo of mass M , i.e. $P(N|M)$, and is hence independent of the individual properties of the galaxies under consideration (e.g. Seljak 2000; Peacock & Smith 2000). A large advance in the development of the HOD function was the recent work of Yang et al. (2003), who focussed attention on the conditional luminosity function, $\Phi(L|M)$: the luminosity function of galaxies in halos of mass M . The CLF extends the HOD by treating galaxies not as indistinguishable objects but as carrying a luminosity ‘label’. This requires an increase in complexity in the model, but allows us to include one of the most important galaxy properties naturally in our models. An alternative formulation would slice the 2D parameter space along the other axis and specify $N(M|L)$ separately for bins of different L . While these are mathematically equivalent, it seems more natural within the halo framework to specify the distribution of L at fixed M rather than the reverse. Guzik & Seljak (2003) suggested an alternative way of including luminosity information in the halo model, which we shall not pursue.

With the CLF, combined with the halo mass function $n(M)$, one can reconstruct the luminosity function

of galaxies:

$$\Phi(L) = \int \Phi(L|M) \frac{dn}{dM} dM = \bar{\rho} \int \frac{\Phi(L|M)}{M} f(\nu) d\nu, \quad (1)$$

where dn/dM is the mass function and $f(\nu)$ is the multiplicity function (see Appendix A). Also the (large-scale, linear) bias of galaxies as a function of luminosity can be computed within this framework:

$$b(L) = \frac{1}{\bar{n}} \int \Phi(L|M) b(M) \frac{dn}{dM} dM, \quad (2)$$

$$= \frac{\bar{\rho}}{\bar{n}} \int \frac{\Phi(L|M)}{M} f(\nu) b(\nu) d\nu. \quad (3)$$

We follow Yang et al. (2003) and model the conditional luminosity function as a Schechter function,

$$\Phi(L|M) dL = \frac{\tilde{\Phi}_*}{\tilde{L}_*} \left(\frac{L}{\tilde{L}_*} \right)^{\tilde{\alpha}} e^{-L/\tilde{L}_*} dL, \quad (4)$$

with the three functions: $\tilde{\alpha}$, \tilde{L}_* and $\tilde{\Phi}_*$. Here the tilde distinguishes these implicit functions of the halo mass, M , from the three parameters of the global luminosity function. The full parameterization of CLF is derived based on arguments about the total mass-to-light ratio of a halo and the characteristic luminosity of a halo.

$$\left\langle \frac{M}{L} \right\rangle (M) = \frac{1}{2} \left(\frac{M}{L} \right)_0 \left[\left(\frac{M}{M_1} \right)^{-\gamma_1} + \left(\frac{M}{M_1} \right)^{\gamma_2} \right], \quad (5)$$

$$\frac{M}{\tilde{L}_*(M)} = \frac{1}{2} \left(\frac{M}{L} \right)_0 f(\tilde{\alpha}) \left[\left(\frac{M}{M_1} \right)^{-\gamma_1} + \left(\frac{M}{M_2} \right)^{\gamma_3} \right]. \quad (6)$$

With the pre-factor,

$$f(\tilde{\alpha}) = \frac{\Gamma(\tilde{\alpha} + 2)}{\Gamma(\tilde{\alpha} + 1, 1)}, \quad (7)$$

introduced to make $N_*(M) = 1$ for small mass halos ($M \ll \min[M_1, M_2]$). The mass-to-light ratio and the typical luminosity are both assumed to have a broken power law form, arguments for which are given in Yang, Mo & van den Bosch (2003).

For $\alpha(M)$, a simple linear function of $\log(M)$ is adopted,

$$\tilde{\alpha}(M) = \alpha_{15} + \eta \log_{10}(M_{15}), \quad (8)$$

with M_{15} the halo mass in units of $10^{15} h^{-1} M_\odot$ and $\alpha_{15} = \tilde{\alpha}(M_{15} = 1)$.

There is a minor problem caused by this definition of $\alpha(M)$ in that the function $f(\alpha)$ becomes divergent when $\alpha \lesssim -1.3$. For negative η this happens at high mass, where $\tilde{L}_*(M) \sim M^{1-\gamma_3}/f(\alpha)$, leading to an unphysical decrease in \tilde{L}_* with increasing mass. The drop in \tilde{L}_* causes a drop in $N(M, L > L_*)$. Fortunately this only happens for very high mass halos which are rare enough that they do not affect the statistical properties which concern us here.

Because the Schechter form is assumed, it can be shown that

$$\langle L \rangle (M) = \int L \Phi(L|M) dL = \tilde{\Phi}_* \tilde{L}_* \Gamma[\tilde{\alpha} + 2], \quad (9)$$

allowing $\tilde{\Phi}_*$ to be derived from the above expressions.

There is an additional parameter M_S which is the mass scale where the local \tilde{L}_* equals the global L_* , i.e.

$$\tilde{L}_*(M_S) = L_* \quad (10)$$

Satisfying this requirement actually sets $(M/L)_0$.

Thus in total there are 8 free parameters in the CLF algorithm: α_{15} , η , M_1 , M_2 , γ_1 , γ_2 , γ_3 , M_S . For a given set of parameters one can reconstruct the luminosity function and luminosity-dependent bias (semi-) analytically. Also the HOD can be computed from

$$N(M, L > L_{\text{cut}}) = \int \Phi(L|M)dL = \Phi_* \Gamma[\alpha + 1, \frac{L_{\text{cut}}}{L_*(M)}]. \quad (11)$$

With the HOD and CLF, we are able to populate an N-body simulation with galaxies and compare the luminosity function, bias and correlation function with observations (see Appendix B).

3. OBSERVATIONAL CONSTRAINTS

In this paper we wish to search for evolution in the way in which galaxies populate halos. We do this by constraining the conditional luminosity function at $z = 0$ and seeing if recent results from DEEP2 allow us to rule out the ‘null hypothesis’ that this CLF is independent of redshift.

Because the observations from these two surveys, and in particular how they relate to the different selection effects inherent in each survey, are so key to this undertaking we review here in some detail the observational constraints we will adopt in our subsequent analysis.

3.1. The Galaxy Surveys

The 2dFGRS (Colless et al. 2001) has recently been completed, having observed redshifts for 230,000 galaxies over ~ 2000 sq. degrees on the sky. The galaxies targeted have been selected to an extinction corrected $b_J < 19.5$ magnitude limit from an updated version of the APM catalogue (Maddox et al. 1990; Maddox, Efstathiou & Sutherland 1990). As will be demonstrated, the sheer size of this data set allows us to rigorously constrain our models at $z \sim 0$ for later propagation to higher redshifts.

The DEEP2 Galaxy Redshift Survey has recently begun to acquire large numbers of galaxy redshifts, and preliminary analyses of the galaxy population and its clustering behavior have recently been published (Coil et al. 2003; Madgwick et al. 2003c). This survey comprises objects selected from CFHT photometry that have been pre-selected to have redshifts $z > 0.7$ (Davis et al. 2002), and is selected to be a magnitude-limited sample based upon the observed r_{AB} magnitudes to $r < 24.1$.

It is clear that, because of the different bands adopted for the magnitude-based selection of the objects in these two surveys (b_J in the 2dFGRS and r_{AB} in DEEP2), they may not in fact probe identical galaxy populations. For this reason we begin by comparing the relative mix of different spectral types in these two surveys before proceeding to describe in more detail the various observational constraints from each.

3.1.1. Selection effects and spectral types

To investigate the relative importance of selection effects in the two surveys, we adopt here the spectral classifications developed for the 2dFGRS and DEEP2 in Madgwick et al. (2002) and Madgwick et al. (2003c) respectively. These classifications, $\eta_{2\text{dF}}$ and η_{DEEP} , have been derived in an analogous way from a principal components analysis (PCA) of the galaxy spectra in each survey and can hence be used to compare the relative mix of different types of galaxies in each survey. The classification itself provides a continuous parameterization of the spectral type of a galaxy based upon the strength of nebular emission present in its rest-frame optical spectrum. It is found that η correlates relatively well with galaxy B -band morphology at $z \sim 0$ (Madgwick 2003). However, the most natural interpretation of η is in terms of the relative amount of star formation occurring in each galaxy (Madgwick et al. 2003a).

In Fig. 1 we compare the distributions of spectral types in the two surveys. It is clear from this comparison that the DEEP2 survey comprises relatively more galaxies that are undergoing recent star-formation (given that it contains proportionately more galaxies with high η values). This is in fact not surprising given the different selection criteria in each survey. In the case of the 2dFGRS, the galaxies have been selected in the observed b_J band – which gives preference to galaxies with recent star formation. However, the observed frame r selection adopted for the DEEP2 galaxies (which are typically $z \sim 1$) in fact corresponds to a rest-frame U -band selection – which is even more biased towards selecting galaxies with recent episodes of star formation.

It is clear from these arguments and Fig. 1 that making a direct comparison between the 2dFGRS and DEEP2 galaxy populations would not give a fair measure of evolution. However those galaxies in the 2dFGRS with more

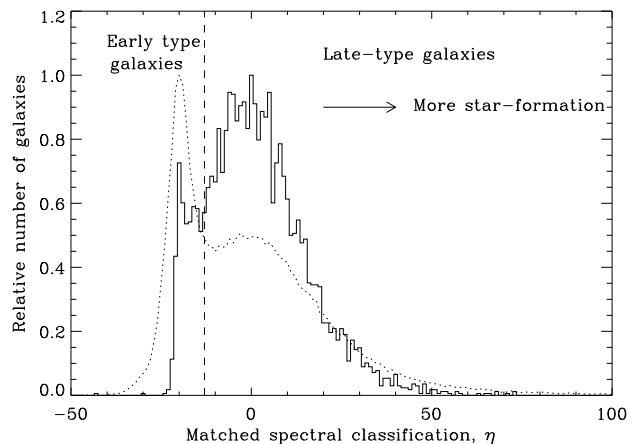


FIG. 1.— The distribution of different types of galaxies in the 2dFGRS and DEEP2 are compared using a ‘matched’ spectral classification (see Madgwick et al. 2003c for details). The dotted histogram shows the distribution of galaxy types from the 2dFGRS and the solid histogram shows that from the DEEP2 Survey. From this comparison we can conclude that the DEEP2 Survey contains a proportionately larger sample of so-called ‘late-type’ galaxies. For this reason in what follows we compare the results from the DEEP2 Survey to those of the late-type 2dFGRS galaxies – as well as for the full 2dFGRS sample.

recent star formation may be a more analogous galaxy population.

In the analysis that follows we perform our fits for both the full 2dFGRS galaxy population (referred to as ‘all’ galaxies) and for just those galaxies with recent star formation (the ‘late-type’ galaxies). In so doing we can effectively bracket the galaxy population that is actually observed in the DEEP2 Redshift Survey¹.

3.1.2. Galaxy clustering

A key element of the analysis presented here is a detailed characterization of the galaxy clustering at both $z = 0$ and $z \sim 1$. At $z = 0$ we have several observational constraints on the two-point correlation function, $\xi(r)$, available to us (e.g. Norberg et al. 2001; Norberg et al. 2002; Hawkins et al. 2003; Madgwick et al. 2003b). Because the actual type of galaxies under consideration appears to be so important to making a fair comparison between the 2dFGRS and DEEP2, we choose to adopt the $\xi(r)$ estimates from Madgwick et al. (2003b), since these have been performed for both ‘early’ and ‘late-type’ galaxies.

In terms of quantifying the degree of clustering at $z \sim 1$ we have a much more limited selection. Coil et al. (2003) have recently presented initial estimates for the correlation function in the DEEP2 Redshift Survey for a variety of different samples. Because this survey occupies such a large range of redshift ($0.7 < z < 1.4$), we choose to adopt the constraints that have been placed on the correlation function over the more limited range $0.7 < z < 0.9$, so that we can neglect evolution within this sample. Specifically we shall assume that $\xi(r)$ is measured at the effective redshift of this sample, as calculated by Coil et al. (2003), $z_{\text{eff}} = 0.8$. We also emphasize that the analysis presented by Coil et al. (2003) made use of only 2219 galaxies drawn from a contiguous sub-region of the initial observations, and hence only represents $\sim 5\%$ of the total potential of the survey. We expect that constraints on the clustering of galaxies at $z \sim 1$ will improve dramatically in the near future.

Note that preliminary estimates of the correlation function have also been made for the types of galaxies in this survey analogous to the 2dFGRS, which would allow us to make much more detailed comparisons in which selection effects would be less important. However, given the small size of the samples available at this early stage no meaningful constraints can be obtained from these calculations.

3.1.3. The luminosity function

The LF provides a fundamental constraint in that it allows us to restrict the number density of galaxies at different epochs. We use here the galaxy LF estimates made by Madgwick et al. (2002), since these have been determined for different sub-samples of galaxy types, which are applicable to the arguments of Sec. 3.1.1. This LF has been fit as a series of step functions (the SWML fit, see Efstathiou, Ellis & Peterson 1988).

An important consideration in fitting to the LF is the fact that the normalization, ϕ_* , of the LF has been determined independently of its shape. The normalization

¹Note that as more data becomes available in the DEEP2 Survey, a much more detailed analysis will become possible, in that we will be able to directly compare observations based upon different types of galaxies in this survey and the 2dFGRS.

of the LF therefore provides a relatively independent constraint on $\phi(L|M)$ and will be treated as such in our analysis.

3.1.4. Absolute bias

The absolute bias, $b(L_*)$, of galaxies in the 2dFGRS has been determined by several authors over a range of different scales (Verde et al. 2002; Lahav et al. 2002; Hawkins et al. 2003). For our purposes we are most interested in the large-scale (linear) bias regime – which is most readily accessible to the analytic model used in the HOD. For this reason we do not adopt the bispectrum analysis presented in Verde et al. (2002), which probes significantly non-linear scales. The determination of b made by Lahav et al. 2002 and Hawkins et al. (2003) are in the fully linear and *quasi*-linear regimes respectively, with the Lahav et al. estimate corresponding to the largest scales. However, we choose to adopt the redshift-distortion based determination of b from Hawkins et al. (2003), since this has also been determined for different types of galaxies (Madgwick et al. 2003b), allowing us to easily extend our analysis to incorporate only the late-type galaxies we expect to dominate in the DEEP2 Redshift Survey.

Given the numerous uncertainties involved in determining $\langle b \rangle$ we choose a conservative value $b(L_*) = 1 \pm 0.2$. As it will turn out the fit already prefers certain values of $b(L_*)$, our loose constraint will not be too critical.

3.1.5. Relative bias

The observed bias is known to vary depending on several aspects of the galaxy population under consideration. Arguably one of the most fundamental variations is the change in relative bias with the intrinsic luminosity of the galaxy population under consideration. Norberg et al. (2001) measured the bias as a function of luminosity, using the clustering of L_* galaxies as a reference point. They found the points can be fitted by a linear relation:

$$b(L, z = 0)/b(L_*, z = 0) = 0.85 + 0.15(L/L_*) \quad . \quad (12)$$

Norberg et al. (2002) found it is the luminosity, not the type, that is the dominant factor causing the variation in the clustering strength. Also, Madgwick et al. (2003b) show that, at large scale, early and late type galaxies have almost the same clustering strength. We will include the luminosity dependence of b , but neglect the type dependence in the following.

4. PARAMETER FITTING

We have in total 9 free parameters that need to be constrained using the results we have listed from the 2dFGRS. For this reason a simple grid-based search of the parameter space is not computationally feasible. Rather we choose to adopt a Markov Chain Monte Carlo (MCMC) method to explore the multi-dimensional space. This has significant computational advantages over a grid-based search and in particular it allows us to more efficiently probe the maximum in the likelihood space.

For every random walk step used by the MCMC, we evaluate its χ^2 using;

1. the observed luminosity function – 22 normalized SWML points between $0.05L_*$ and $5L_*$;

2. the relative bias points in 6 luminosity bins and a rough estimate of the absolute bias $b(L_*)$;
3. the four priors we have added (§4.1).

We will additionally incorporate constraints from the observed correlation functions after the MCMC has been completed using an ‘importance re-sampling’ of the chain, as described later (§4.2).

Note that because the normalization and the shape of the luminosity function provide relatively independent constraints, we want to treat them separately. So, we fix the normalization of the analytically computed points by the SWML luminosity bin nearest to L_* , $\hat{\Phi}(L_*)$, i.e.

$$\phi(L_i) = \Phi(L_i) \frac{\hat{\Phi}(L_*)}{\hat{\Phi}(L_*)}, \quad (13)$$

We then sum the χ^2 of the remaining $N_l - 1$ computed $\phi(L_i)$ points using SWML points and error bars. This way we get the χ^2 of the shape of the luminosity function. For the normalization, it’s not determined as accurate as the shape. We set $\hat{\Phi}(L_*)$ to have a fractional error of 10% around the observed value $\hat{\Phi}(L_*)$.

For the bias, since the observational results are given in relative bias already, we do not need to do the same thing as we did for luminosity function. However, we do need to incorporate the χ^2 of the absolute bias.

The χ^2 is evaluated through the following equation.

$$\chi^2 = \chi_{\hat{\Phi}}^2 + \chi_b^2 + \chi_{\text{priors}}^2, \quad (14)$$

where the first two terms are;

$$\chi_{\hat{\Phi}}^2 = \frac{3}{N_l - 1} \sum_{i=1}^{N_l} \left[\frac{\hat{\Phi}(L_i) - \phi(L_i)}{\Delta \hat{\Phi}(L_i)} \right]^2 + \left[\frac{\hat{\Phi}(L_*) - \Phi(L_*)}{0.1 \hat{\Phi}(L_*)} \right]^2, \quad (15)$$

and

$$\chi_b^2 = \frac{1}{N_b} \sum_{i=1}^{N_b} \left[\frac{\hat{b}(L_i) - b(L_i)}{\Delta \hat{b}(L_i)} \right]^2 + \left[\frac{b(L_*) - 1}{0.2} \right]^2. \quad (16)$$

Here $\hat{\Phi}(L_i)$ and \hat{b} are observed quantities and all symbols without a ‘hat’ are analytically computed quantities. We give the shape of the luminosity function a relative weight 3 since it is measured with much less uncertainty than other constraints we used. As it turns out the constraint $b(L_*) = 1 \pm 0.2$ is not really needed as the fit will provide a tighter constraint.

The chain is started from the model used in Yang, Mo & van den Bosch (2003) and is then allowed a ‘burn-in’ period for the chain to equilibrate in the likelihood space. The cosmology used in the code is the same as in the simulation. At any point in the chain we generate a new trial element by drawing parameter shifts from independent Gaussian distributions in each of the nine CLF parameters. The probability of accepting a new random walk step is taken to be

$$P_{\text{accept}} = \begin{cases} 1.0 & \text{for } \chi_{\text{new}}^2 < \chi_{\text{old}}^2 \\ \exp [-(\chi_{\text{new}}^2 - \chi_{\text{old}}^2)/2] & \text{for } \chi_{\text{new}}^2 > \chi_{\text{old}}^2 \end{cases} \quad (17)$$

Given the sampling strategy we adopted, the acceptance rate is around 25%, leading to nearly independent samples in the chain after a (few) thousand elements. We ran four chains, with different random number seeds, each for 100,000 steps. The χ^2 does not decrease very much from the initial guess, indicating that the starting model is within the equilibrium region of the chain.

4.1. Priors

The CLF formalism has a ‘free’ function for halos of every mass. Even given the restriction to Schechter forms this requires us to choose three free functions of mass ($\tilde{\alpha}$, \tilde{L}_* and $\tilde{\Phi}$) to specify the model, and further parameterizing these functions as (double) power laws still allows a great deal of freedom.

Unfortunately, we have found that it is possible to obtain reasonable $\Phi(L)$ and $b(L)$ for ‘pathological’ $N(M, L > L_{\text{cut}})$. For example, the number of galaxies brighter than the local $\tilde{L}_*(M)$ in a halo of mass M is proportional to $M^{\gamma_3 - \gamma_2}$. If γ_2 becomes larger than γ_3 and $\tilde{L}_*(M)$ does not increase fast enough to compensate, the number of galaxies brighter than (the global) L_* in a halo of mass M will decrease for $M \gg \max[M_1, M_2]$.

To eliminate these and other instabilities we have chosen to apply some priors on $N(M)$. In most cases the pathological models would be rejected by comparing the predicted and observed correlation functions (see §4.2), however we include those constraints after the chain has been run. In this sense one can consider our priors as a way to increase the efficiency of our procedure.

After extensive experimentation we found that the following additional priors worked quite well in our analysis. First we apply a Gaussian prior that $\alpha_{15} = -1.0 \pm 0.2$ to ensure that only negative values of α_{15} are adopted by the chain. Without this prior positive values of α_{15} occur quite regularly, despite being unphysical. In particular, we have based this prior upon composite observations of the Coma cluster LF by Driver & De Propris (2002), who have derived a faint-end slope of $\alpha = -1.01^{+0.04}_{-0.05}$, for this cluster. We allow more flexibility in our constraint than this, to allow for the fact that this is only a rough constraint on our model.

We also provide two priors on the shape of $N(M)$, both log-normal. The first sets $\hat{N}(10^{15} h^{-1} M_{\odot})$ to a fiducial value with a factor of 5 (1σ) error and the second provides a similar constraint on $\hat{N}(10^{12} h^{-1} M_{\odot})$. After the importance resampling described in §4.2 the distributions of \hat{N}_{15} and \hat{N}_{12} are both much narrower than the imposed priors, indicating that the exact form is not important.

Our last prior provides a constraint on the number of galaxies residing in halos of very low mass. This prior has been included for both theoretical and practical reasons and again the distribution in the chain after importance resampling (§4.2) is much narrower than the prior. Theoretically we believe that even low luminosity galaxies do not live in very low mass halos, $M \ll 10^{10} h^{-1} M_{\odot}$, and we wish to encode this information in the fit. The practical reason is that our N-body simulation has limited mass resolution which makes it impossible for us to compute $\xi(r)$ for such models. Mathematically the problematic models arise when L_* does not decline fast enough

with mass. In this situation many of the fainter galaxies can reside in halos of mass smaller than $10^{10} h^{-1} M_{\odot}$. Even though $N(M, > 0.1L_*)$ is in the range 10^{-4} to 10^{-3} for these halos, their huge number ensures a significant contribution to the total number of galaxies. We require $L_*(M = 10^{10} h^{-1} M_{\odot}) < 0.02L_*$ so that almost no $0.1L_*$ galaxies live in halos with $M < 10^{10} h^{-1} M_{\odot}$.

4.2. Importance re-sampling

The MCMC calculated so far has adopted only the constraints from the 2dFGRS LF and biasing results to constrain the CLF at $z \sim 0$. In fact there is substantially more information available to us in the form of very accurate determinations of the two-point correlation function, $\xi(r)$.

It is possible to directly relate the CLF to the correlation function analytically, by making various assumptions about the way halos and galaxies are distributed relative to each other (e.g. Peacock & Smith 2000; Seljak 2000; Magliocchetti & Porciani 2003; Zehavi et al. 2003). However, given that we have detailed N-body simulations available to us, we instead choose to populate these using the CLF and then calculate $\xi(r)$ estimates from these.

Using the N-body simulations instead of analytic approximations to the halo profiles and clustering allows us to make much more detailed comparisons to the shape of the correlation functions, which is particularly appealing given the very high fidelity of these observations.

One immediate drawback of calculating the correlation function from the N-body simulations (instead of purely analytically), is the additional computational time required. Given that the MCMC has yielded a chain of 400,000 elements, the calculation of $\xi(r)$ for each of these is infeasible. Fortunately it is also unnecessary, as the distribution of $\xi(r)$ can be obtained from a smaller set of samples. We choose 200 models, (given that only one in every few thousand elements is completely independent), at random, from the chain and compute $\xi(r)$ for each of these, for the ‘all galaxy’ and ‘late-type’ samples at $z = 0.1$ and $z = 0.8$ (the effective redshifts of the 2dFGRS and DEEP2 $\xi(r)$ calculations). We then adopt an ‘importance re-sampling’ technique (Gilks, Richardson & Spiegelhalter 1996) to include the goodness-of-fit between the models and the observed 2dFGRS correlation function. We only fit $\xi(r)$ over the range $0.2 < r < 3 h^{-1} \text{Mpc}$, since for separations $r < 200 h^{-1} \text{kpc}$ fibre collisions lead to a decrease in the observed 2dFGRS $\xi(r)$ (see e.g. Hawkins et al. 2003), and for $r > 3 h^{-1} \text{Mpc}$ our N-body simulations become susceptible to finite box size effects.

4.3. Results

Once the importance re-sampling is incorporated then all the necessary $z \sim 0$ observational constraints have been included in our CLF determination and the parameter space can be reviewed. In particular, we compare in the left panel of Fig. 2 the *mean* correlation functions derived from our fitted CLFs and N-body simulations to their corresponding observed $\xi(r)$ from the 2dFGRS. It can be seen from this figure that the models have very successfully fitted both the correlation function of the ‘late-type’ and ‘all galaxy’ 2dFGRS samples.

The mean HODs derived from our model CLFs are shown in Fig. 3. In this particular plot we show the mean

number of $L > 0.1L_*$ galaxies occupying a halo of the specified mass. This particular luminosity cut is the one we have adopted throughout this analysis, as it is found to correspond well to the observed distributions of luminosities in the two surveys.

It can be seen from Fig. 3 that the two CLFs predict very similar low-mass cut-offs in the HOD, but have very different behavior at high masses. Clearly star forming galaxies appear to dominate the galaxies within low mass halos, but become successively more under-represented in the highest mass halos. This result is certainly not surprising given observed morphology-density relations (e.g. Dressler 1980), however it is interesting to see the effect quantified in this way.

A different way of plotting the CLF is to instead relate the probability that a galaxy within a specified range of luminosities inhabits a dark matter halo of a given mass. This is also shown in Fig. 3, for both the ‘all galaxy’ and ‘late-type’ samples. A similar plot appeared in Yang et al. (2003) for a single representative model, our procedure allows us to also include the uncertainty in the model parameters in a statistically correct manner.

5. CONSTRAINING GALAXY EVOLUTION

Our preliminary analysis is complete, in that we have successfully constrained the CLF formulation of the halo-model to the observations of the 2dFGRS. In so doing we have had to make only the most basic prior assumptions suggesting that the observational data is more than adequate to tightly constrain this model.

The next step in our analysis is to determine the degree of inference we can make as to the evolution in the galaxy population to redshift $z \sim 0.8$, by contrasting the predictions of this constrained model to the preliminary results from the DEEP2 Redshift Survey.

5.1. Reconstructing the DEEP2 $\xi(r)$

As discussed previously, the DEEP2 correlation function, $\xi(r)$, has been determined in Coil et al. (2003), and it is this estimate that we now try to recover from our CLF models. In particular, we use the $\xi(r)$ estimated over the redshift interval $0.7 < z < 0.9$ which has an effective redshift $z_{\text{eff}} = 0.8$.

The simplest assumption we can make in propagating our model to higher redshifts, is that the CLF has not changed between $z = 0.1$ and $z = 0.8$. In order to test this assumption we again turn to our N-body simulations, which allow us to extrapolate the dark matter halo distribution to $z = 0.8$. these simulations can then be repopulated and the correlation functions recalculated.

The results of this analysis are presented in the right panel of Fig. 2, where the mean N-body $\xi(r)$ is shown for both the ‘late-type’ and ‘all galaxy’ CLFs (after importance re-sampling with respect to the 2dFGRS correlation functions at $z = 0.1$), propagated to redshift $z = 0.8$. The fractional uncertainty is 20%, independent of scale. What is remarkable from this figure is the fact that the predicted correlation function at $z = 0.8$ from our fitted CLFs is completely consistent with that which has been observed in the DEEP2 Survey – especially for the late-type 2dFGRS galaxy sample which probably corresponds more closely to the galaxies observed in the DEEP2 Redshift Survey (see §3.1.1). The agreement could be even

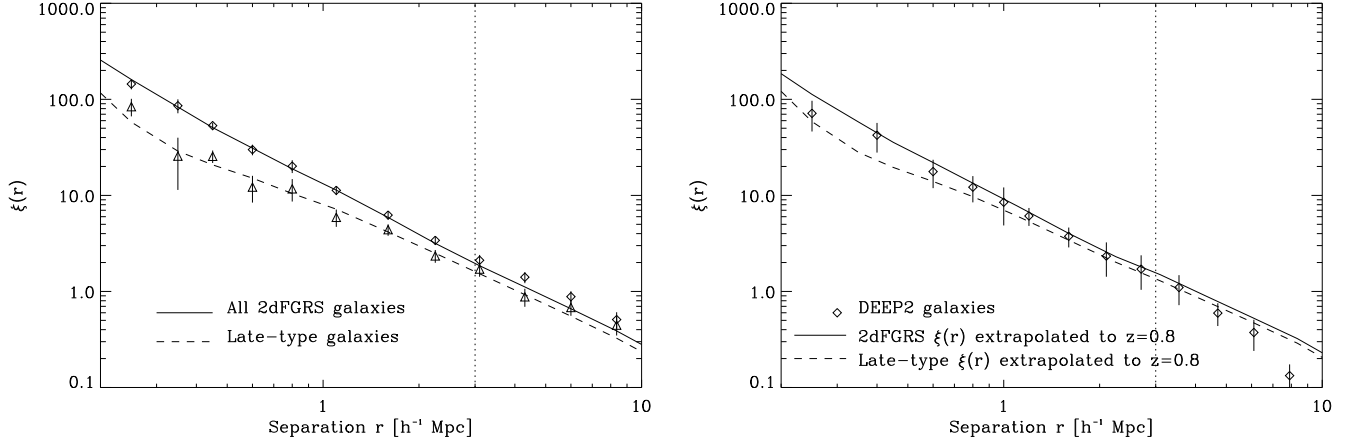


FIG. 2.— The left panel shows the mean correlation functions after performing importance re-sampling on the model CLFs fit to the 2dFGRS for ‘late-type’ (dashed line) and ‘all’ (solid line) galaxies. It can be seen that our models can recover the observed $\xi(r)$ in great detail. In each plot, the dotted vertical line at $r = 3 h^{-1}$ Mpc shows the maximum separation over which our $\xi(r)$ estimates from the N-body simulations are robust. The right panel shows the correlation function calculated using the DEEP2 Redshift Survey (points), and compares this with the mean correlation functions, derived from the same model CLFs used in the left panel (after extrapolating the N-body simulations to $z = 0.8$). The agreement between the mean model CLF $\xi(r)$ ’s at $z = 0.8$ and the observed DEEP2 $\xi(r)$ is very good and quite unexpected. This result suggests that we cannot rule out the null-hypothesis of no evolution in the halo model between redshifts $z = 0.1$ and $z = 0.8$.

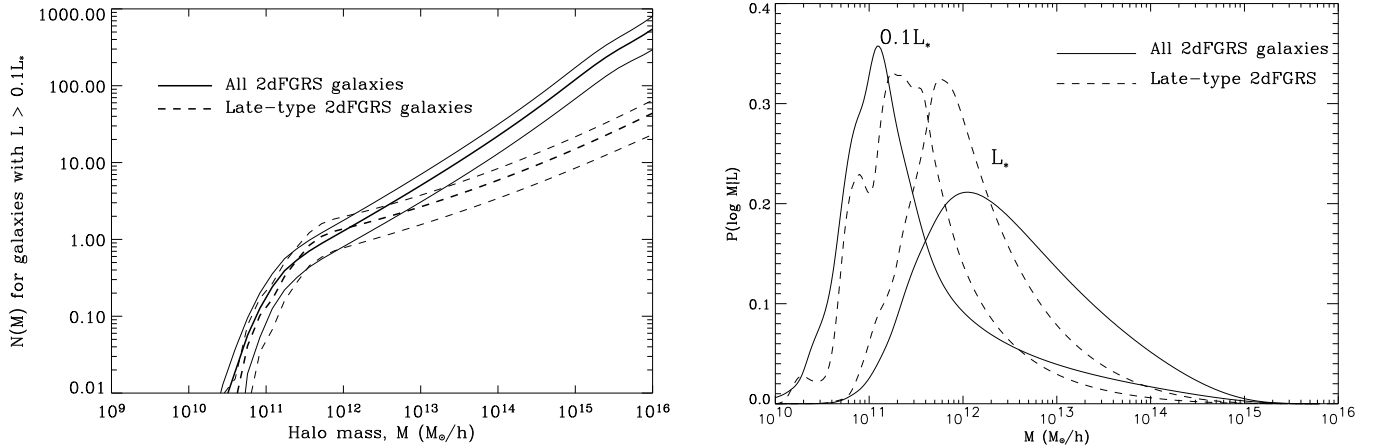


FIG. 3.— The mean HOD, $N(M)$, is shown for galaxies with $L > 0.1L_*$ (thick lines; left panel), as derived from the CLFs after importance re-sampling to fit the observed 2dFGRS correlation function. The variance at each mass is indicated by the thinner lines bracketing the central one. It can be seen that the late-type galaxies appear to dominate low mass halos, but become steadily more under-represented in higher mass halos. The right panel shows how we can invert this to derive the probability that a galaxy with a given range of luminosity inhabits a halo of mass, M . This function, $P(M|L)$, is shown here for both $0.1L_*$ and L_* galaxies, the solid lines again correspond to the ‘all galaxies’ sample and the dashed lines to the ‘late-type’ sample.

better than shown in Fig. 2 if we account for the effects of mask making on the DEEP2 data points at small scales ($< 300 h^{-1}\text{kpc}$) and finite field effects at larger scales.

This result is extremely surprising, in that it appears to imply that we cannot rule out an unevolving halo model to $z \sim 1$: the galaxies observed in the DEEP2 Redshift Survey appear to inhabit their parent dark matter halos in the same way as those observed in the 2dFGRS. Had the cut-off in $N(M, > 0.1L_*)$ evolved to higher masses we would have seen a steepening in $\xi(r)$ on sub-Mpc scales. Also, had the $N < 1$ tail of $N(M, > 0.1L_*)$ extended over a broader mass range at $z \sim 1$ than $z \sim 0$ we would have seen a suppression of $\xi(r)$ on sub-Mpc scales. Similarly, steepening the high- M slope of $N(M)$ increases the bias, which is not observed.

It is difficult to place precise limits on what functional forms are allowed because of the limited amount of data, the uncertainty in the underlying cosmological model and the large dimensional space in which we are working (with its associated degeneracies). As a rough gauge of sensitivity, increases in the mass cut-off by even an order of magnitude are strongly disfavored as is steepening $N(M)$ to $N \propto M$. We defer a more thorough analysis until more data become available.

5.2. Other predictions for the DEEP2 Survey

Given that the CLF does not appear to evolve significantly at high redshifts, it is now possible to make a series of predictions relating to what we expect to see in the DEEP2 Survey as more data becomes available. We briefly describe a handful of these predictions in this section.

5.2.1. The luminosity function

The evolution of the LF is perhaps one of the most natural outputs of the conditional luminosity function. Given that we can accurately trace the dark matter halo mass function through N-body simulations, Eqn. 1 provides a simple link between the two.

We have calculated the expected LF at $z = 0.8$, given the constraints placed on the CLF from the 2dFGRS observations. Interestingly it shows little evolution – only a small variation in the faint-end slope, α , and the characteristic luminosity, L_* , are seen to $z = 0.8$. This is an interesting result which suggests that our hypothesis of a non-evolving CLF also implies little evolution in the *relative* distribution of luminosities of galaxies. Note that our clustering analysis has been determined entirely in terms of relative luminosities (L/L_*) so evolution in the absolute value of L_* is not constrained. In fact, given that we expect the distribution of galaxies to be relatively established by $z = 0.8$ (as would be expected for no evolution in the CLF), a purely *passive* change in L_* would be entirely consistent with our results. Such a change would be brought about by e.g. the internal dimming of the galaxies as their stellar populations became successively older and fainter. However, our prediction of the distribution of luminosities relative to L_* should be robust, and so for this reason we predict that little evolution in the faint end slope of the LF will be seen in the DEEP2 Survey, when compared to the 2dFGRS. Once a detailed calculation of the DEEP2 LF becomes available we will pursue this possibility in more detail.

5.2.2. Luminosity dependent bias

The average bias at $z \sim 0$ has a luminosity dependence close to that reported by Norberg et al. (2001), since these data were used in the fit. Overall we find that the bias is determined by the data to 2% for $L \ll L_*$ and 5% for $L \gg L_*$, both much stronger constraints than our prior on b . We can then ask how the mean bias relation evolves with redshift, again assuming that the CLF is independent of z . By $z = 0.8$ the mean bias has risen 30%, and the variance across the chain is between 5-9% depending on L . The luminosity dependence has steepened from 0.15 to ~ 0.25 as shown in Table 1.

6. CONCLUSIONS

In this paper we have attempted to constrain the degree of evolution in the way galaxies inhabit their parent dark matter halos by contrasting the very accurate observations of the galaxy population in the 2dFGRS (at $z \sim 0$) to preliminary results from the DEEP2 Redshift Survey at $z = 0.8$. In order to do so we have had to carefully consider the fidelity of the different observational results available for this analysis and how these relate to the different selection effects in each survey.

Based upon a comparison between the types of galaxies observed in each survey, we were able to conclude that the DEEP2 Redshift Survey contains a much larger fraction of ‘late-type’ galaxies i.e. those currently under-going significant amounts of star formation. For this reason we have attempted to not only contrast this survey with the full 2dFGRS, but also with observational results based upon only the ‘late-type’, star forming galaxies in this survey. In this way we believe we are able to make a much more fair comparison between the two surveys, in that we can effectively ‘bracket’ the population observed in the DEEP2 Redshift Survey. Note that as more data becomes available in the DEEP2 Survey, this bracketing will no longer be necessary as we will be able to directly compare the different types of galaxies in each survey.

A great deal more observational results are available at $z = 0$ than at $z \sim 1$, and for this reason we have decided to adopt the approach of making the most detailed fit possible of the HOD at $z = 0$, and to then test how consistent this HOD was to preliminary clustering results at $z = 0.8$. In so doing we were able to show that the current observation of the correlation function at $z = 0.8$ is remarkably consistent with no evolution in the HOD to this redshift.

This result is very surprising. The HOD quantifies the impact of galaxy formation and interaction processes

L/L_*	$b(z = 0.1)$	$b(z = 0.8)$
0.3	0.94 ± 0.03	1.13 ± 0.05
0.7	1.02 ± 0.03	1.26 ± 0.05
1.0	1.08 ± 0.04	1.34 ± 0.06
1.5	1.18 ± 0.05	1.48 ± 0.09

TABLE 1

THE LARGE-SCALE, LINEAR THEORY BIAS AT $z = 0$ AND $z = 0.8$ FROM OUR IMPORTANCE RESAMPLED CHAINS FOR ALL GALAXIES. THE MEAN AND VARIANCE DEFINED BY THE 200 ELEMENTS IN THE CHAIN ARE REPORTED.

present in the galaxy population, and in particular how this relates to the underlying dark-matter halo distribution. Our results suggest that there has in fact been no change in the way galaxies are distributed in their host dark-matter halos over approximately half the age of the Universe.

At present our results are preliminary, in that the correlation function of galaxies at $z = 0.8$ is still relatively poorly constrained. In addition, the absence of an estimated luminosity function for this population makes a more detailed comparison of the evolutionary processes difficult. However, as the DEEP2 Redshift Survey continues to increase its sample size we expect these issues to be resolved so that much more conclusive remarks can be made. In addition, as the sample size increases, correlation functions for different types of galaxies in the DEEP2 Redshift Survey will become available, which will allow us to be much more precise about the importance of galaxy type selection in our results.

Other improvements to our analysis will be forthcoming when results from the recently begun VLT-VIRMOS Redshift Survey (Le Fevre et al. 1999) become available. This survey comprises an I_{AB} -selected sampling of the galaxy population at similar redshifts to the DEEP2 Redshift Survey, which at these redshifts is much more comparable to a rest-frame B -selection of galaxies. For this reason the incorporation of this survey into our analysis should allow us to more accurately address the issues of sample selection and to what degree these impact our conclusions.

We would like to thank Marc Davis, Brian Gerke and Joanne Cohn for helpful discussions, and Alison Coil for providing the DEEP2 correlation function in electronic format. M.W. would like to thank Ravi Sheth and Andreas Berlind, and D.S.M. thanks Shaun Cole for numerous enlightening discussions on the halo model. The simulations used here were performed on the IBM-SP at the National Energy Research Scientific Computing Center. This research was supported by the NSF and NASA.

REFERENCES

- Bennett C.L., et al., 2003, ApJ, in press [astro-ph/0302207]
 Benson A.J., et al., 2000, MNRAS, 311, 793
 Berlind A., Weinberg D.H., 2002, ApJ, 575, 587 [astro-ph/0109001]
 Coil A., et al. (*the DEEP2 Team*), 2003, ApJ, submitted [astro-ph/0305586]
 Cole S., Kaiser N., 1989, MNRAS, 237, 1127
 Cole S., Aragon-Salamanca A., Frenk C.S., Navarro J.F., Zepf S.E., 1994, MNRAS, 271, 781
 Colless M. M., et al. (*the 2dFGRS Team*), 2001, MNRAS, 328, 1039 [astro-ph/0106498]
 Cooray A., Sheth R., 2002, Physics Reports, 372, 1 [astro-ph/0206508]
 Davis M., Efstathiou G., Frenk C.S., White S.D.M., 1985, ApJ, 292, 371
 Davis M., et al., (*the DEEP2 Team*) 2002, SPIE, [astro-ph/0209419]
 De Propriis R., Driver S. P., 2002, JENAM2002 Galaxy Evolution Workshop [astro-ph/0212520]
 Dressler A. 1980, ApJ, 236, 351
 Efstathiou G., Ellis R.S., Peterson B.A., 1988, MNRAS, 232, 431
 Efstathiou G., Frenk C.S., White S.D.M., Davis M., 1988, MNRAS, 235, 715
 Gardner, J.P., Katz, N., Hernquist, L., Weinberg, D.H., 2001, ApJ, 559, 131
 Gilks W.R., Richarson S., Spiegelhalter D.J., 1996, Markov Chain Monte Carlo in practice (London: Chapman and Hall).
 Guzik J., Seljak U., 2003, MNRAS in press [astro-ph/0201448]

- Hawkins E., et al., (*the 2dFGRS Team*) 2003, MNRAS, submitted [astro-ph/0212375]
 Jing Y.P., Mo H.J., Borner G., 1998, ApJ, 494, 1 [astro-ph/9708115]
 Kauffmann G., White S.D.M., Guiderdoni B., 1993, MNRAS, 264, 201
 Katz N., Hernquist L., Weinberg D.H., 1999, ApJ, 523, 463 [astro-ph/9806257]
 Lahav O., et al. (*the 2dFGRS Team*), 2002, mnras, 333, 961 [astro-ph/0112162]
 Le Fevre, O., et al., 1999, ASP, Vol. 176, 250
 Ma C.-P., Fry J. N., 2000, ApJ, 543, 503
 Maddox S. J., Efstathiou G., Sutherland W. J., Loveday J., 1990, MNRAS, 243, 692
 Maddox S. J., Efstathiou G., Sutherland W. J., 1990, MNRAS, 246, 433
 Madgwick D. S. et al., (*the 2dFGRS Team*) 2002, MNRAS, 333, 133 [astro-ph/0107197]
 Madgwick D. S., 2003, MNRAS, 338, 197 [astro-ph/0209051]
 Madgwick, D. S., Somerville, R., Lahav, O., Ellis, R. S., 2003a, MNRAS, in press [astro-ph/0210471]
 Madgwick D.S. et al., (*the 2dFGRS Team*) 2003b, MNRAS, in press [astro-ph/0303668]
 Madgwick D.S. et al., (*the DEEP2 Team*) 2003c, ApJ, submitted [astro-ph/0305587]
 Mo H.-J., White S.D.M., 1996, MNRAS, 282, 347
 Norberg P., et al., 2001, MNRAS, 328, 64 [astro-ph/0105500]
 Norberg P., et al., 2002, MNRAS, 332, 827 [astro-ph/0112043]
 Peacock J.A., Smith R.E., 2000, MNRAS, 318, 1144 [astro-ph/0005010]
 Pearce, F.R. et al., 1999, ApJ, 521, 99 [astro-ph/9905160]
 Magglicchetti M., Porciani C., 2003, MNRAS submitted [astro-ph/0304003]
 Press W.H., Schechter P., 1974, ApJ, 187, 452
 Scoccimarro R., Sheth R., 2001, MNRAS, 329, 629 [astro-ph/0106120]
 Scoccimarro R., Sheth R., Hui L., & Jain B., 2001, ApJ, 546, 20 [astro-ph/0006319]
 Scranton R., 2002, MNRAS, 332, 697 [0108266]
 Seljak U., 2000, MNRAS, 318, 203 [astro-ph/0001493]
 Sheth R., Tormen G., 1999, MNRAS, 308, 119 [astro-ph/9901122]
 Smith R.E., et al., 2003, MNRAS, 341, 1311 [astro-ph/0207664]
 Somerville R., Primack J., 1999, MNRAS, 310, 1087 [astro-ph/9802268]
 Strauss M. A., et al. (*the SDSS collaboration*), 2002, AJ, 124, 1810 [astro-ph/0206225]
 Verde L., et al. (*the 2dFGRS Team*), 2002, MNRAS, 335, 432 [0112161]
 White M., 2001, MNRAS, 321, 1 [astro-ph/0005085]
 White M., Hernquist L., Springel V., 2001, ApJ, 550, L129 [astro-ph/0012518]
 White S.D.M., Rees M., 1978, MNRAS, 183, 341
 White M., 2002, ApJS, 579, 16 [astro-ph/0207185]
 Yang X., Mo H.-J., van den Bosch F.C., 2003, MNRAS, 339, 1057 [astro-ph/0207019]
 Yang X., Mo H.-J., van den Bosch F.C., Chu Y., 2003, MNRAS submitted [astro-ph/0303524]
 Yoshikawa K., Taruya A., Jing Y.P., Suto Y., 2001, ApJ, 558, 520
 Zehavi I., Weinberg D.H., Zheng Z., Berlind A.A., Frieman J.A., et al., 2003, ApJ submitted [astro-ph/0301280]

APPENDIX

THE HALO MODEL

In this appendix we describe the details of the halo model formalism that we use in the main paper. A review of the halo model, with reference to the original literature, can be found in Cooray & Sheth (2002).

The halo mass function, dn/dM , describes the (comoving) number density of halos with mass in the interval $[M, M + dM]$. This function depends on the redshift and the power spectrum of dark matter halos as well as the underlying cosmology. Typically one adopts a change of variables, to give a dimensionless form of this function in terms of the halo peak height ν . Specifically, the multiplicity function, $f(\nu)$, is used since this is independent of cosmology. The relation between this multiplicity function

and the halo mass function is simply given by,

$$\frac{\bar{\rho}}{M} f(\nu) d\nu = \frac{dn}{dM} dM. \quad (\text{A1})$$

where $\bar{\rho}$ is the mean matter density of the Universe, and the cosmology dependence resides entirely in the peak height definition,

$$\nu \equiv [\delta_c(z)/\sigma(M)]^2. \quad (\text{A2})$$

Note that many authors use $\nu = \delta_c(z)/\sigma(M)$ rather than its square as we have done here. Here $\delta_c \simeq 1.868$ is a threshold parameter taken from the theory of spherical top-hat collapse while $\sigma(M)$ is the rms mass fluctuation within spheres of radius $R = [M/(4\pi\bar{\rho}/3)]^{1/3}$ evaluated in linear theory, at redshift z . For the multiplicity function, $f(\nu)$, we use the ‘ST’ form, motivated by ellipsoidal collapse and fit to N-body simulations (Sheth & Tormen 1999):

$$\nu f(\nu) = A(1 + \nu'^{-p})\nu'^{1/2}e^{-\nu'/2}, \quad (\text{A3})$$

where $p = 0.3$ and $\nu' = 0.707\nu$. The constant A determines the normalization and is fixed by the requirement that all the mass lie in a given halo,

$$\frac{1}{\bar{\rho}} \int M \frac{dn}{dM} dM = \int f(\nu) d\nu = 1. \quad (\text{A4})$$

We can regain the older Press & Schechter (1974) expression by taking $\nu' = \nu$ and $p = 0$.

Halos within some mass range $[M, M + dM]$ are biased tracers of the underlying matter distribution. To linear order the bias can be computed from the peak-background split (Efstathiou et al. 1988; Cole & Kaiser 1989; Mo & White 1996) which for the ST mass function gives,

$$b(\nu) = 1 + \frac{\nu' - 1}{\delta_c} + \frac{2p}{\delta_c(1 + \nu'^p)}. \quad (\text{A5})$$

This bias is appropriate for very large scales where the bias is expected to be deterministic, linear and scale independent. Note that this scheme automatically satisfies the requirement that the mean bias of mass is unity:

$$\langle b \rangle_{\text{mass}} = \int b(\nu) f(\nu) d\nu = 1. \quad (\text{A6})$$

Given a HOD function $\langle N \rangle(M)$ we can use the mass function and halo biasing scheme described above to easily compute the mean galaxy bias (which is defined as the scale independent linear bias of galaxy relative to mass),

$$\langle b \rangle_g = \frac{\bar{\rho}}{\bar{n}} \int \frac{\langle N \rangle}{M} f(\nu) b(\nu) d\nu. \quad (\text{A7})$$

Note that \bar{n} is the mean density of galaxies, and can be computed from,

$$\bar{n} = \int \langle N \rangle \frac{dn}{dM} dM = \bar{\rho} \int \frac{\langle N \rangle}{M} f(\nu) d\nu. \quad (\text{A8})$$

GALAXY CATALOGUES

To compute the correlation function given the CLF we make use of a large N-body simulation of a Λ CDM model. The simulation employs 512^3 particles in a periodic, cubic box of side $128 h^{-1} \text{Mpc}$ and was run with the *TreePM* code described in White (2002). The cosmological model was chosen to provide a reasonable fit to a wide range of observations with $\Omega_m = 0.3$, $\Omega_\Lambda = 0.7$, $H_0 = 100 h \text{ km s}^{-1} \text{Mpc}^{-1}$ with $h = 0.7$, $\Omega_B h^2 = 0.02$, $n = 0.95$ and $\sigma_8 = 0.9$ (close to the best fit to the CMB data for this cosmology). The gravitational force softening was of a spline form, with a ‘Plummer-equivalent’ softening length of $9 h^{-1} \text{kpc}$ comoving. The particle mass is $1.3 \times 10^9 h^{-1} M_\odot$. The simulation was started at $z = 100$ and evolved to the present with the full phase space distribution dumped every $128 h^{-1} \text{Mpc}$ from $z \simeq 3$ to $z = 0$. As a check on finite volume effects we compared our results to those from a similar simulation in a box with force softening and box side twice as large, with $8 \times$ more massive particles. It is based on this comparison that we restrict our fits to $r < 3 h^{-1} \text{Mpc}$.

We use outputs at redshifts appropriate to the 2dF ($z \simeq 0.1$) and DEEP2 ($z \simeq 0.8$) surveys. For each output we produce a halo catalogue by running a ‘friends-of-friends’ group finder (e.g. Davis et al. 1985) with a linking length $b = 0.15$ (in units of the mean inter-particle spacing). This procedure partitions the particles into equivalence classes, by linking together all particle pairs separated by less than a distance b . We keep all halos with more than 8 particles, and consider each of these halos as a candidate for hosting ‘galaxies’.

We populate the simulation with ‘galaxies’ by marking certain simulation particles and assigning them luminosities. The HOD function computed from the CLF model gives the mean number of galaxies (more luminous than some L_{cut}) which would be in a halo of mass M . The halo mass is estimated as the sum of the masses of the particles in the FoF halo, times a small correction factor which provides the best fit to the Sheth-Tormen mass function (Sheth & Tormen 1999). An actual number of galaxies is drawn from a distribution for each halo in the simulation, and we use the nearby integer distribution.

Once the number of galaxies in each halo is known, they are assigned luminosities from $\Phi(L|M)$. The most luminous galaxy is assigned to the center of mass of the halo, and the other galaxies are assigned to random particles within the halo. While the code allows the possibility of a radial or velocity bias in assigning galaxies to particles, throughout we assumed that galaxies traced the mass and velocity distribution of the halo (inheriting its shape and any substructure).

Given the total number of galaxies brighter than L_{cut} in each halo it is necessary to choose luminosities for them based on $\Phi(L|M)$. Just as it was necessary to specify both $\langle N \rangle$ and the higher moments above, it is necessary to know the fluctuations about the mean $\Phi(L|M)$ at this stage. If the luminosities of galaxies each halo are drawn independently from $\Phi(L|M)$ then one occasionally finds relatively low mass halos with two ‘bright’ galaxies. Since such systems have small radii this in turns implies an increase in the ‘bright’ galaxy correlation function at small scales. Such an increase can indeed be seen in some of the

semi-analytic models, but appears to be absent in data. This suggests that some mechanism acts to suppress pairs of bright galaxies in small halos. We can model this in a number of ways. On one extreme we could calculate the luminosities for all galaxies in halos of similar masses by drawing from $\Phi(L|M)$ and then distribute them, round-robin, in halos in order of decreasing luminosity. This ensures that all the bright galaxies are partitioned among the halos rather than having pairs end up in any one halo. A slightly different approach, which has very similar clustering properties, was suggested by Yang et al. (2003). Here we compute L_1 such that a halo of mass M has (on average) only 1 galaxy brighter than L_1 . We then draw luminosities for the galaxies in this halo, allowing only the brightest galaxy to have $L \geq L_1$. This also suppresses the higher moments of $\Phi(L|M)$ for bright galaxies. We shall follow Yang et al. (2003) unless stated otherwise.